Towards naturalistic human neuroscience and neuroengineering: behavior mining in long-term video and neural recordings

Satpreet H. Singh¹, Steven M. Peterson¹, Rajesh P. N. Rao¹ and Bingni W. Brunton¹

¹University of Washington

{satsingh, stepeter}@uw.edu, rao@cs.washington.edu, bbrunton@uw.edu*

Abstract

Recent advances in brain recording technology and artificial intelligence are propelling a new paradigm in neuroscience beyond the traditional controlled experiment. Naturalistic neuroscience studies neural computations associated with spontaneous behaviors performed in unconstrained settings. Analyzing such unstructured data lacking a priori experimental design remains a significant challenge, especially when the data is multi-modal and longterm. Here we describe an automated approach for analyzing large (\approx 250 GB/subject) datasets of simultaneously recorded human electrocorticography (ECoG) and naturalistic behavior video data for 12 subjects. Our pipeline discovers and annotates thousands of instances of human upper-limb movement events in long-term (7–9 day) naturalistic behavior data using a combination of computer vision, discrete latent-variable modeling, and string pattern-matching. Analysis of the simultaneously recorded brain data uncovers neural signatures of movement that corroborate prior findings from traditional controlled experiments. We also prototype a decoder for a movement initiation detection task to demonstrate the efficacy of our pipeline as a source of training data for brain-computer interfacing applications. We plan to publish our curated dataset, which captures naturalistic neural and behavioral variability at a scale not previously available. We believe this data will enable further research on models of neural function and decoding that incorporate such naturalistic variability and perform more robustly in real-world settings.

1 Introduction

While controlled experiments have been highly successful in informing our understanding of brain function, neuroscientists have always been interested in studying brain activity associated with spontaneous behaviors in freely behaving subjects. Hypotheses regarding brain function have typically been tested using carefully designed, well-controlled

experimental tasks, where timing of cues, stimuli, and behavioral responses are known precisely. Recent technological advances have enabled us to study increasingly naturalistic and longer brain recordings, giving rise to a new paradigm called "naturalistic neuroscience" [Huk et al., 2018; Gabriel et al., 2019; Markowitz et al., 2018; Wang et al., 2016] where neural computations associated with such spontaneous behaviors are studied. Analyzing such unstructured, long-term, and multi-modal data poses a substantial challenge, due in part to the lack of a priori experimental design and the difficulty of isolating interpretable behavioral events.

1.1 Our approach

We present a scalable behavior-mining approach to analyze simultaneously recorded naturalistic brain and behavior data, obtained from human subjects undergoing long-term monitoring in a hospital prior to epilepsy surgery. Our video processing pipeline (Figure 1) starts with estimating the locations of several keypoints on a subject's body. We then segment each keypoint's trajectory in time using discrete latentvariable models, building a discretized representation of pose dynamics. Interestingly, having a discrete, sequential representation of upper-limb pose simplifies the problem of detecting behavioral events to pattern-matching on strings. Using regular-expressions corresponding to patterns of interest, we discover thousands of interpretable events per subject—an order of magnitude more observations than in a typical controlled human experiment. To study the rich naturalistic variability associated with these events, we also extract metadata including movement angle, magnitude, and duration.

Next, we explore the use of these behavioral events for neuroscience and neuroengineering applications by analyzing the simultaneously recorded brain data. Event-averaged spectrograms associated with our naturalistic human upperlimb movement initiation events corroborate and strengthen previous findings from controlled experiments [Miller *et al.*, 2007]. Preliminary investigations also suggest that our workflow could produce data useful for training brain-computer interface (BCI) decoders; due to the use of training data representative of naturalistic variability, such decoders may perform more robustly in real-world deployments.

^{*}Address correspondence to BWB

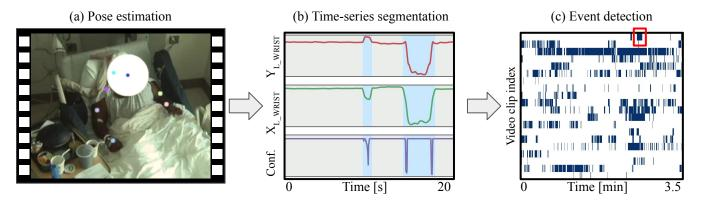


Figure 1: Pipeline for behavioral video data processing: (a) Video frame showing estimated pose keypoints (colored dots) on human subject. (b) Autoregressive hidden Markov model (Section 4.2) robustly segments pose trajectory into *rest* (shaded grey) and *move* (shaded light blue) states. (c) Raster plot of pose states (*move* in dark blue, *rest* in white) for several video-clips for pattern matching at scale. Red box depicts one *movement initiation* event matching a pattern of 15 contiguous *rest* states (0.5s) followed by 15 contiguous *move* states (0.5s).

1.2 Our contributions

- We present a highly automated, novel workflow for analyzing simultaneously recorded naturalistic long-term human brain and behavioral video data.
- We develop a domain-relevant, robust, temporally precise, and queryable representation of human upper-limb pose.
- To showcase our workflow, we provide example applications in neuroscience and neuroengineering, suggesting that our approach and results are of broad interest.
- Finally, to facilitate further research in this area, we will release our curated dataset consisting of annotated naturalistic events and associated neural recordings.

2 Related work

Many recent methodological innovations have addressed the automated analysis of non-human animal behavior [Batty et al., 2019; Mathis et al., 2018; Johnson et al., 2016; Wiltschko et al., 2015] (see also [Mathis and Mathis, 2020] for a recent survey and [Anderson and Perona, 2014] for a perspective on this emerging area). A typical non-human naturalistic neuroscience experiment [Johnson et al., 2019; Markowitz et al., 2018; Berman, 2018] first collects simultaneously recorded behavioral video and neural activity data from one or more freely behaving subjects in an uncontrolled but sufficiently confined environment. Next, the video recordings are processed through an extensive pipeline consisting of steps such as: segmenting the subject(s) from the background, transforming subject pose to common coordinates using affine transformations, estimating pose or tracking positions of body-parts across frames, and higher-level operations such as classifying pose or segmenting pose into actions. Combined with the simultaneously recorded neural data, such naturalistic behavior data are being used to shed light on previously unanswerable questions in behavioral neuroscience, often at unprecedented scale.

Human action-recognition methods from mainstream computer vision [Ramasamy Ramamurthy and Roy, 2018] are relevant but not directly applicable to the needs of naturalistic human neuroscience. Traditionally, action-recognition

research has concerned itself with discriminating activities at a coarse level, such as sitting vs. walking, and has often assumed the availability of a large corpus of labeled training data. In contrast, to study the kinds of behaviors that interest neuroscientists and neuroengineers, we seek to localize fine-grained movements to sub-second temporal resolution, and ideally use the fewest behavioral labels possible. Lastly, since it is not known which behaviors or behavioral characteristics will elicit neural responses worth studying further, a queryable representation that permits the flexibility to study several kinds of behaviors is desirable. Recent work by [Fu et al., 2019] develops such representations for semi-automated exploration of scenes in general videos.

Our work is most closely related to recent work in human naturalistic neuroscience. [Gabriel et al., 2019] uses optical flow to detect coarse limb movements from video taken in a similar clinical setting as ours and develops neural decoders for detecting these from brain data. [Chen et al., 2018] develops a toolbox for human pose-estimation in such clinical environments. [Wang et al., 2018] uses similar video data and pose-estimation to extract joint trajectories on which movements are detected using a moving window heuristic. Compared to Wang et al. (2018), we take a more principled approach to modeling pose data, which allows us to localize movement events with fine temporalresolution and characterize entire movement trajectories. In addition, we exceed the aforementioned studies taken together in the number of subjects analyzed. Other related but less relevant work in this area include [Alasfour et al., 2019; Wang et al., 2016].

3 Data collection

Our dataset consists of human intracranial electrocorticography (ECoG) neural recordings and simultaneously recorded behavior video, obtained opportunistically from 12 consenting epilepsy patients for the entire duration of each patient's long-term (7–10 days) continuous clinical observation. Patient behavior is continuously recorded by a wall-mounted camera (RGB/infrared 640×480 pixel) for real-time mon-

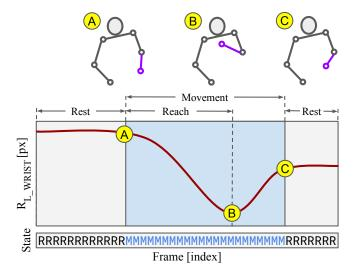


Figure 2: Schematic of metadata extraction: [Above] Cartoon showing left-hand movement at time of (A) movement initiation (B) maximum displacement from initiation (reach) and (C) movement end. [Below] Time course of left-wrist radial distance [pixels], and discretized state (R: rest, M: move). Extracted movement metadata include duration, start and end coordinates, among others (Sec. 4.4).

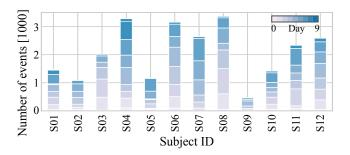


Figure 3: Number of right-wrist movement initiation events discovered per day for each of 12 subjects, totaling 465 to 3482 events per subject across their entire duration of clinical observation (255 \pm 118 s.d. per day).

itoring by an around-the-clock clinical team and only turned off or panned away during private times. Patients perform their daily activities (talking, eating, watching TV, using a computer or phone, sleeping, receiving clinical care etc.) while being tethered to a brain-recording interface.

Each patient has ≈ 90 electrodes implanted under the skull and directly on their brain surface, including an 8×8 grid-electrode. These cover different cortical regions predominantly in one brain hemisphere as determined by individual clinical need (left hemisphere for 7 patients). To simplify interpretability, we restrict our analysis to only the ≈ 64 grid electrodes in this paper. We also do not analyze brain data from the first two days of a patient's hospital stay, since patients are typically heavily medicated while recovering from surgery, making the data neurally and behaviorally atypical. Sampling rates for video and ECoG are 30 fps and 1000 Hz respectively. Together, the ECoG and video (≈ 18 million frames for a week) total about 250 GB of data per patient.

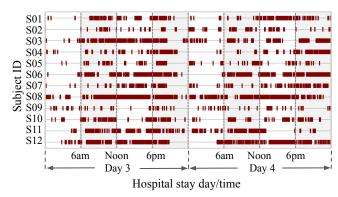


Figure 4: Raster plot of right-wrist movement initiation event occurrences showing bursts of activity interspersed with periods of rest or blacklisted (Section 4.1) periods.

4 Behavioral video processing pipeline

We develop and validate a pipeline to extract temporally precise, interpretable movement events, by processing the video data through pose-estimation, pose time-series segmentation, event detection and finally, event metadata extraction (Fig. 1).

4.1 Markerless pose estimation

To extract a subject's pose from raw video, we train a state-of-the-art markerless pose estimation tool [Mathis *et al.*, 2018] known for its speed and data efficiency [Nath *et al.*, 2019]. For training data, we manually annotate ≈ 1000 frames per subject chosen randomly from the entire duration of a subject's video data, preferentially sampling active, daytime hours over times when the subject was asleep. For each frame, we annotate up to 9 keypoints on the subject's body whenever visible. These include the nose, both wrists, elbows, shoulders, and ears (Figure 1a).

The pose-estimation tool produces the (x,y) coordinates and a confidence estimate between [0,1] for each keypoint per frame (Figure 1b). We observe good training performance $(1.54\pm0.13 \text{ s.d.})$ pixels RMS error) and holdout set performance $(5.97\pm1.96 \text{ s.d.})$ pixels RMS error; holdout is 5% of manual annotations, excluding points below confidence threshold of 0.1). For approximate scale, 12 pixels in the video are about 4 real-world cms (about the width of a human wrist). On average, estimating pose for the entire duration of a subject's video took 400 GPU-hours per subject using AWS p2.16xlarge NVIDIA K80 GPUs.

As a final post-processing step, we denoise the estimated pose trajectories by median filtering (window length 11 frames) and smoothing (window length 11, 2nd order Savitzky-Golay filter). We also quickly label the activity in the video data at a coarse (every ≈ 3 minute) level of granularity to create a *blacklist* that is excluded from further processing. This blacklist includes long time-spans of sleep, times when a clinical or research team is actively working with the subject, private times, and times when pose-estimation is impossible due to severe occlusion of the subject's body.

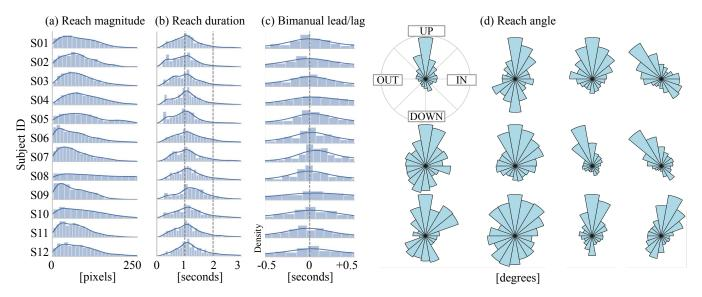


Figure 5: Histograms of right-wrist movement initiation event metadata per subject for their entire duration of clinical observation: (a) Reach magnitude shows a dominance of small movements, (b) Reach durations tend to be concentrated around ≈1s, (c) When both hands move together ("bimanually"), they tend to start at about the same time. (d) Polar histograms show that many subjects primarily make upward-downward reaches. However, reaches in almost every other direction are also observed.

4.2 Pose time-series segmentation

Next, we segment the pose time-series in a temporally precise manner into discrete, interpretable states. We apply a first-order autoregressive hidden semi-Markov model (ARHSMM) with two latent states to each keypoint's time-series (Figure 1b for left-wrist). Similar to [Wiltschko et al., 2015], we fit the ARHSMM using the pyhsmm-autoregressive Python package. This model converts each keypoint's continuous pose dynamics into discretized dynamics consisting of rest and move states. The resulting states are at frame-rate resolution and is robust to variation in lighting, camera pan and angle, and level of activity in the video. Using a semi-Markov, rather than a Markov, model accounts for the bias that limbs tend to be at rest most of the time and mitigates unnecessary switching between latent states.

4.3 Behavioral event mining

Discretizing the pose trajectories facilitates the description of scientifically interesting behaviors performed spontaneously by the subject, even though they vary greatly in duration. Specifically, the problem of finding different types of behavioral **events** reduces to string pattern matching on the discretized dynamics. For the behaviors we explore in the rest of this paper, we look for *movement initiation* events by matching a pattern of 15 consecutive *rest* states (0.5s), followed by at least 15 consecutive *move* states (0.5s). Similarly, *no-movement* events are state sequences of 90 *rest* states (3.0s) across both wrists and the nose. To create our database of wrist movements, we use regular expressions to quickly find thousands of non-overlapping instances of such patterns in the discretized pose dynamics for each subject.

4.4 Event metadata extraction

For each instance of movement event, we further describe several metadata features from the continuous posedynamics associated with each movement event. This includes movement-associated metadata (Figure 2) like the (x,y) coordinates of the keypoint at the start and end of the event, duration of the entire movement (up to next rest state), and rest duration before and after movement.

Naturalistic hand movements are often made to reach out, grab an object, then bring it back towards the body. Thus, we define the *reach* of a wrist movement to be its maximum radial displacement during the course of the event, as calculated from its location at the start of the event. We extract the *magnitude*, *angle*, and *duration* for each reach.

To measure the *shape* of a movement, we fit 1^{st} , 2^{nd} and 3^{rd} -degree polynomials to a keypoint's displacement trajectory. Differences between the quality of the fit (as measured by R^2) to each polynomial type provide a rough measure of the "curviness" of the movement trajectory. We also estimate a movement's onset and offset *speeds*, by calculating the keypoint's displacement change within short time windows around the start and end of the movement.

Since people often move both hands at the same time, we annotate each of our wrist movement events with metadata about the opposing wrist's movement, if any. By juxtaposing the discrete state sequence of both wrists, we calculate when the opposing hand starts to move (*lead/lag time difference*) and how long this movement overlaps with that of the primary hand (*overlap duration*).

False positives in event discovery still exist at this stage due to pose estimation failures and unusual pose states. To compensate for failures in 2D pose estimation, we calculate movement-weighted *confidence* scores for each event and remove those below a manually determined threshold. To

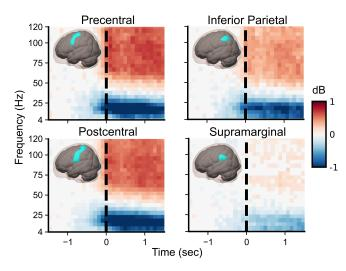


Figure 6: Neural correlates of movement initiation: Event-locked spectrograms, averaged by brain region across 12 subjects, show movement-associated high-frequency power increase and low-frequency power decrease. These patterns corroborate and strengthen previous findings from controlled experiments [Miller *et al.*, 2007].

eliminate outlier pose states, we calculate mean *distance* and mean *angle* between *shoulder* keypoints, then remove events from the top and bottom 5 percentiles of these quantities.

5 Characterizing naturalistic events

On executing our pipeline on all 12 subjects, we find a wide variation between subjects in the number of events discovered by our automated procedure (Figure 3). This variability can primarily be attributed to inter-subject differences in cycles of sleep and wakeful activity, and clinical treatment regimes (Figure 4). We also observe rich within-subject variability in the event metadata (Figure 5), which differentiates our dataset from those collected in controlled experiments. Since our subjects receive no instructions for when and how to move, we expect that the observed movement statistics will closely reflect the natural statistics of human upper-limb movement.

6 Towards naturalistic neuroscience and neuroengineering

We use the event data produced by our naturalistic event generation pipeline towards two example applications.

6.1 Application: Neural encoding

How behaviors are encoded by the coordinated activation of brain regions is a core scientific question in systems neuroscience. To examine the neural correlates of naturalistic movement initiation, we perform a standard time-frequency (TF) analysis [Cohen, 2014] by averaging event-locked spectrograms for each subject, using hundreds of movement initiation events picked to match movement statistics (reach magnitude, onset velocity, and shape) of a previous controlled experimental study [Miller *et al.*, 2007].

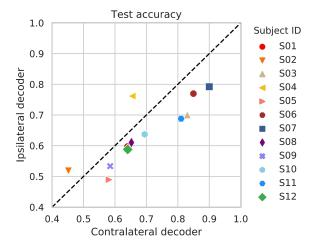


Figure 7: Decoding accuracy for initiation of movement of contralateral (side opposite electrode implant) and ipsilateral (same side) wrists: As expected, decoding of contralateral movements is slightly more accurate than ipsilateral in almost all cases.

Encoding results In Figure 6, we observe movementassociated power increases in a high-frequency band (76-100 Hz) and decreases in a low-frequency band (8–32 Hz) across many cortical areas in our event-averaged TF spectrograms; this pattern is similar to what was observed with controlled experimental trials in Miller et al. (2007). Furthermore, we strengthen prior findings by showing that these movement-associated patterns hold across 5 days, well beyond the timescale of a typical controlled experiment (less than hours). To the best of our knowledge, this is the first reported instance of a TF analysis of spontaneous naturalistic movements using events discovered by an automated workflow. We elaborate on these results in our concurrently released preprint (anonymous for now), where we investigate the consequences of the relatively higher variance of naturalistic movement statistics, and model the contributions of the various movement metadata to the observed neural responses.

6.2 Application: Neural decoding

A grand challenge in the field of neuroengineering is to develop BCIs that can be used to predict spontaneous activity and intentions in everyday settings [Smalley, 2019]. Here we perform a preliminary study on the use of our pipeline as a source of training data for a BCI decoder that detects wrist movement initiation events. Specifically, we train separate classifiers, tailored to each subject, to discriminate between movement initiation events and no-movement epochs for each wrist using only features derived from the ECoG neural recordings.

Classifier specifications

Our decoder uses the Random Forest (RF) algorithm [Breiman, 2001], which is typically considered one of the best off-the-shelf classification algorithms for small/medium sized datasets [Hastie *et al.*, 2009]. We apply standard preprocessing steps to the ECoG data [Gabriel *et al.*, 2019; Miller *et al.*, 2007; Schalk *et al.*, 2007], including 60-Hz

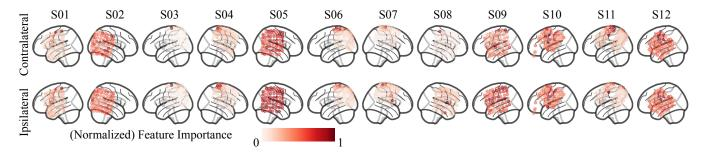


Figure 8: Decoder feature importance scores aggregated by electrode, showing spatial contributions of different brain regions. Scores are normalized by dividing by highest electrode score for each decoder. Electrode coverage over motor cortex is highly correlated with decoder accuracy; for instance, subjects having good motor cortex coverage (S07, S06, S03 and S11) have the highest decoding performance (Fig. 7).

line noise removal, large-amplitude artifact removal, mediancentering using a common reference across all electrodes, and standardization by dividing by individual electrode variance. Using ECoG data 0.5s before to 0.5s after each event, we compute TF spectrograms at each of the 64 grid electrodes and use the flattened vector of TF bins as features for the classifier (TF bins are $200 \text{ms} \times 5 \text{Hz}$ resolution, truncated at 150 Hz; ≈ 9600 features total).

Given that the brain's response drifts over the course of days, a reduced subset of events from 3 consecutive days (typically days 3 through 5 of clinical monitoring) are used in the dataset, with events from the last day serving as the test set. To eliminate the confound of movement initiation in the opposing wrist, we further filter events to exclude those with significant rest to move transitions in the opposing wrist within the ± 0.5 s window used for ECoG data. Positive (movement initiation) and negative (no-movement) examples are balanced by down-sampling negative examples. This eliminates bias in the training set and sets up a baseline performance of 50% accuracy for test set performance. Training and test supports are 644 \pm 439 s.d., and 340 \pm 195 s.d. examples respectively. We tune the RF using a 20-sample randomized search over two hyperparameters: number of trees (range: [50, 250]) and maximum tree-depth (range: [3, 15]). For each set of hyperparameters, 5-fold cross-validation holdout accuracy is used to measure performance. Final performance reported in Figures 7 and 8 is from training using best hyperparameters and correspond to classifier accuracy on events from the withheld test day.

Decoding results

Individual subject classifier performance (Figure 7) is comparable to previously reported work [Gabriel *et al.*, 2019; Wang *et al.*, 2018] but varies widely between subjects, correlated with differences in motor cortex coverage (Fig. 8).

Due to hemispheric lateralization of brain function, decoding contralateral limb movements is expected to be easier than decoding ipsilateral movements [Tam et al., 2019]. Our decoding accuracy on the test set (Fig. 7) tends to be higher for the contralateral wrist in almost all cases. Since false positives (FPs) in the event data establish a ceiling on classifier accuracy, we estimate their prevalence by manually inspecting 100 randomly sampled events per event-type from each subject $(5.2\% \pm 4.6\% \text{ s.d.})$ for no-movement, $24.8\% \pm 4.6\% \text{ s.d.}$

11.0% s.d. for contralateral, and $16.0\% \pm 8.5\%$ s.d. for ipsilateral events). With more stringent rejection of FPs, we expect improved decoding performance and potentially more pronounced differences between contralateral and ipsilateral decoding accuracy.

Feature importance scores [Breiman, 2001; Hastie *et al.*, 2009] aggregated by electrode provide *rough* measures of the spatial contribution of various brain areas (Figure 8). Electrodes covering the motor cortex, when available, dominate feature importance (e.g. Subjects S07, S06, S03 and S11 in Fig. 7). When motor cortex coverage is limited or unavailable, inter-region correlations known to exist in the brain [Tam *et al.*, 2019; Miller *et al.*, 2007; Schalk *et al.*, 2007] are exploited by the classifier but with limited decoding capacity.

7 Discussion

In summary, we develop a highly automated and scalable approach for analyzing long-term datasets of simultaneously collected human brain and naturalistic behavior data. We demonstrate two example applications of the dataset we produce: examining neural correlates of movement, and decoding of naturalistic movement initiation from brain data. Key to the success of our applications is the ability to extract a large number of repeated instances of movement initiation events with high temporal precision, an essential requirement for generating event-averaged spectrograms [Cohen, 2014]. The ability to select movements by magnitude, onset velocity, and complexity (using shape metadata) allowed us to match movement statistics between naturalistic and controlled experimental data, enabling a fair comparison. Furthermore, being able to select events without opposing wrist activity allowed us to eliminate confounds when comparing movement decoders for opposing wrists.

A primary drawback of our dataset is that our estimated pose-coordinates are 2D projections. Our dataset could be made significantly richer by using a stereoscopic camera system that would enable pose-estimation and object-tracking to take place in 3D. Controlling false positives in the event discovery process is also an area where improvements could deliver significant performance gains.

We are exploring several extensions enabled by this work. These include building decoders for various event metadata, representation learning to obtain the specific neural encodings of movement attributes, transfer learning to adapt decoders

trained for one subject to another, and latent-factor modeling of the variability and non-stationarity of the brain data. We will publish our dataset, which we hope will facilitate future research at the intersection of AI and neuroscience¹.

Acknowledgements

We would like to thank the following individuals for helpful discussions: Nancy X. R. Wang, James Wu, Nile Wilson, Jeffery G. Ojemann, Ariel Rokem, Kameron D. Harris, Renshu Gu, David J. Caldwell, and Preston Jiang. We thank John So for extensive help with manual annotations.

This work was funded by NSF award (1630178) and DOD/DARPA award (FA8750-18-2-0259) to BWB and RPNR, by NSF award EEC-1028725 to RPNR, the Alfred P. Sloan Foundation (BWB), and the Washington Research Foundation (BWB).

¹Per conference rules, no link to dataset included at this time.

References

- [Alasfour *et al.*, 2019] A Alasfour, P Gabriel, X Jiang, I Shamie, L Melloni, T Thesen, P Dugan, D Friedman, W Doyle, O Devinsky, et al. Coarse behavioral context decoding. *Journal of Neural Engineering*, 16(1):016021, 2019.
- [Anderson and Perona, 2014] DJ Anderson and P Perona. Toward a Science of Computational Ethology. *Neuron*, 84(1):18–31, October 2014.
- [Batty et al., 2019] E Batty, M Whiteway, S Saxena, D Biderman, T Abe, S Musall, W Gillis, J Markowitz, A Churchland, JP Cunningham, et al. Behavenet: nonlinear embedding and bayesian neural decoding of behavioral videos. In *Advances in Neural Information Processing Systems*, pages 15680–15691, 2019.
- [Berman, 2018] GJ Berman. Measuring behavior across scales. *BMC Biology*, 16(1), December 2018.
- [Breiman, 2001] L Breiman. Random forests. *Mach. Learn.*, 45(1):5–32, October 2001.
- [Chen et al., 2018] K Chen, P Gabriel, A Alasfour, C Gong, W K Doyle, O Devinsky, D Friedman, P Dugan, L Melloni, T Thesen, D Gonda, S Sattar, S Wang, and V Gilja. Patient-Specific Pose Estimation in Clinical Environments. IEEE Journal of Translational Engineering in Health and Medicine, 6:1–11, 2018.
- [Cohen, 2014] MX Cohen. Analyzing Neural Time Series Data: Theory and Practice. MIT Press, January 2014.
- [Fu et al., 2019] DY Fu, W Crichton, J Hong, X Yao, H Zhang, A Truong, A Narayan, M Agrawala, C Ré, and K Fatahalian. Rekall: Specifying Video Events using Compositions of Spatiotemporal Labels. arXiv:1910.02993 [cs], October 2019.
- [Gabriel et al., 2019] PG Gabriel, KJ Chen, A Alasfour, T Pailla, WK Doyle, O Devinsky, D Friedman, P Dugan, L Melloni, T Thesen, D Gonda, S Sattar, SG Wang, and V Gilja. Neural Correlates of Unstructured Motor Behaviors. *Journal of Neural Engineering*, 16(6):066026, October 2019.
- [Hastie *et al.*, 2009] T Hastie, R Tibshirani, and J Friedman. The elements of statistical learning: data mining, inference, and prediction, Springer Series in Statistics, 2009.
- [Huk et al., 2018] A Huk, K Bonnen, and BJ He. Beyond Trial-Based Paradigms: Continuous Behavior, Ongoing Neural Activity, and Natural Stimuli. *The Journal of Neu*roscience, pages 1920–17, July 2018.
- [Johnson et al., 2016] MJ Johnson, DK Duvenaud, A Wiltschko, RP Adams, and SR Datta. Composing graphical models with neural networks for structured representations and fast inference. In Advances in Neural Information Processing Systems 29, pages 2946–2954. Curran Associates, Inc., 2016.
- [Johnson *et al.*, 2019] RE Johnson, S Linderman, T Panier, CL Wee, W Song, KJ Herrera, A Miller, and F Engert. Probabilistic models of larval zebrafish behavior reveal structure on many scales. *Current Biology*, 2019.

- [Markowitz et al., 2018] JE Markowitz, WF Gillis, CC Beron, SQ Neufeld, K Robertson, ND Bhagat, RE Peterson, E Peterson, M Hyun, SW Linderman, BL Sabatini, and SR Datta. The Striatum Organizes 3D Behavior via Moment-to-Moment Action Selection. Cell, 174(1):44–58.e17, June 2018.
- [Mathis and Mathis, 2020] MW Mathis and A Mathis. Deep learning tools for the measurement of animal behavior in neuroscience. *Current Opinion in Neurobiology*, 60:1–11, 2020.
- [Mathis *et al.*, 2018] A Mathis, P Mamidanna, KM Cury, T Abe, VN Murthy, MW Mathis, and M Bethge. DeepLab-Cut: Markerless pose estimation of user-defined body parts with deep learning. Technical report, Nature Publishing Group, 2018.
- [Miller *et al.*, 2007] KJ Miller, EC Leuthardt, G Schalk, RPN Rao, NR Anderson, DW Moran, JW Miller, and JG Ojemann. Spectral Changes in Cortical Surface Potentials during Motor Movement. *Journal of Neuroscience*, 27(9):2424–2432, February 2007.
- [Nath *et al.*, 2019] T Nath, A Mathis, AC Chen, A Patel, M Bethge, and MW Mathis. Using DeepLabCut for 3D markerless pose estimation across species and behaviors. *Nature protocols*, 14:2152–2176, 2019.
- [Ramasamy Ramamurthy and Roy, 2018] S Ramasamy Ramamurthy and N Roy. Recent trends in machine learning for human activity recognition A survey. Wiley Interdisciplinary Reviews: Data Mining and Knowledge Discovery, 8(4):e1254, 2018.
- [Schalk et al., 2007] G Schalk, J Kubanek, KJ Miller, NR Anderson, EC Leuthardt, JG Ojemann, D Limbrick, D Moran, LA Gerhardt, and JR Wolpaw. Decoding twodimensional movement trajectories using electrocorticographic signals in humans. *Journal of Neural Engineering*, 4(3):264, 2007.
- [Smalley, 2019] E Smalley. The business of brain-computer interfaces. *Nature biotechnology*, 37(9):978, 2019.
- [Tam et al., 2019] W Tam, T Wu, Q Zhao, E Keefer, and Z Yang. Human motor decoding from neural signals: a review. BMC Biomedical Engineering, 1(1):22, 2019.
- [Wang et al., 2016] NXR Wang, JD Olson, JG Ojemann, RPN Rao, and BW Brunton. Unsupervised Decoding of Long-Term, Naturalistic Human Neural Recordings with Automated Video and Audio Annotations. Frontiers in Human Neuroscience, 10, April 2016.
- [Wang et al., 2018] NXR Wang, A Farhadi, RPN Rao, and BW Brunton. AJILE movement prediction: Multimodal deep learning for natural human neural recordings and video. In *Thirty-Second AAAI Conference on Artificial Intelligence*, 2018.
- [Wiltschko et al., 2015] AB Wiltschko, MJ Johnson, G Iurilli, RE Peterson, JM Katon, SL Pashkovski, VE Abraira, RP Adams, and SR Datta. Mapping Sub-Second Structure in Mouse Behavior. Neuron, 88(6):1121–1135, December 2015.